CHAPTER- III

MATERIALS, EXPERIMENTAL PROGRAM, METHODS, AND TEST PROCEDURES

3.1 INTRODUCTION

The quantity of coal ash produced every year creates a huge amount of accumulation near the ash disposal location. These disposal locations are not properly designed to sustain such huge loads that give rise to the failure of such dams due to the deposition of consecutive layers every year. In order to minimize the disastrous effect of coal ash on the environment, a new practical application area/material must be proposed. The present study specifically concentrated on the application of fly ash as pavement subgrade or embankment fill material. The pavement construction involves a considerable amount of capital, therefore a complete study is required under static and dynamic loading conditions before the application of fly ash in the field. Therefore, to achieve successful implementation, the objectives of the present study were divided into four phases a) identification of chemical, morphological, and mineralogical content, b) geotechnical characterization, c) dynamic characterization, and d) small-strain shear modulus characterization of the considered materials. These four experimental phases will help in the selection of the present material for a particular application. This chapter discussed about the complete experimental testing program that needs to be carried out to fulfill the objectives of the present study. These experimental testing were first

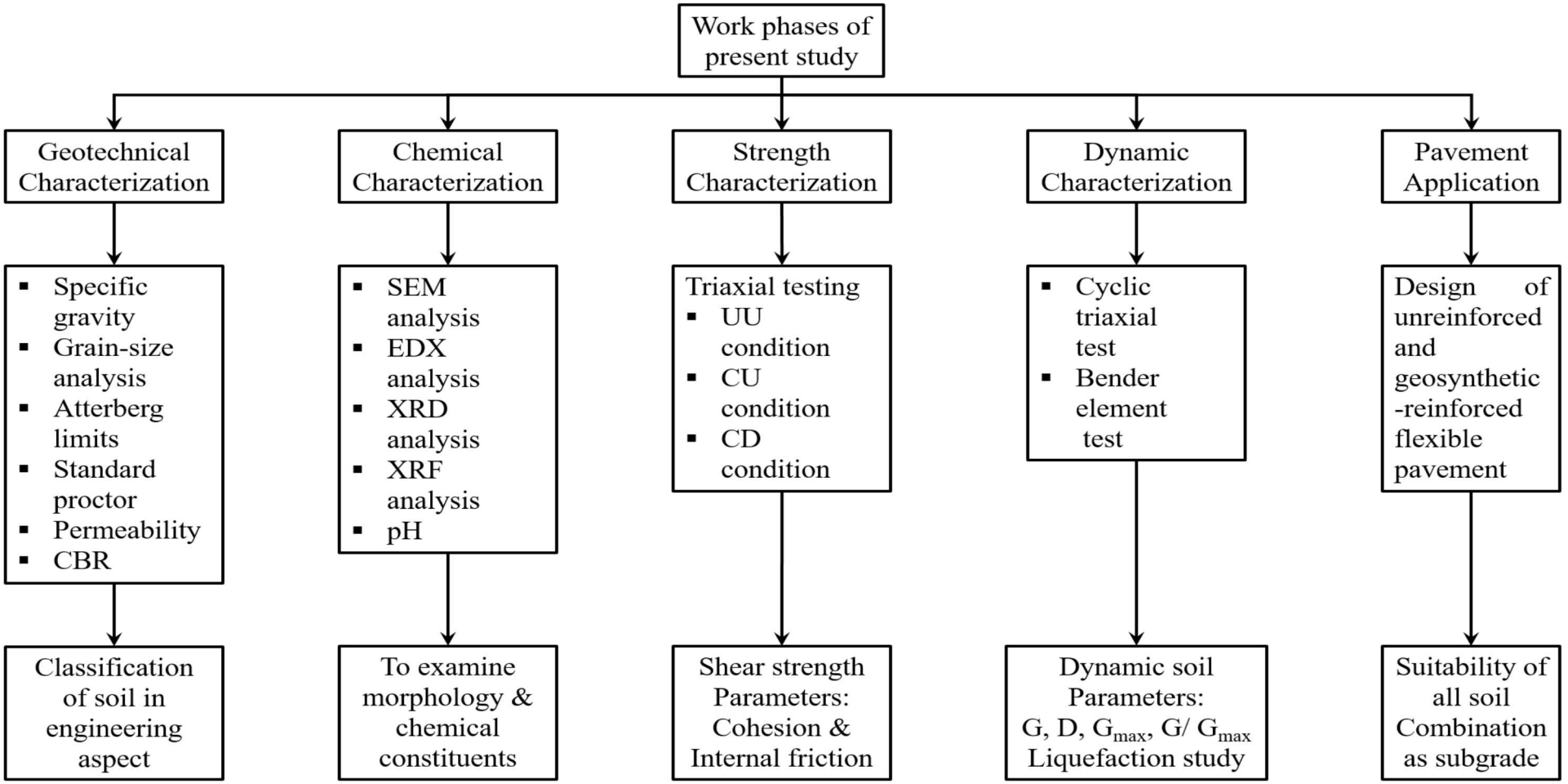

Fig. 3.1. Flowchart of the experimental and analytical evaluation of present soil combinations under different phases.

executed with chemical characterization, followed by geotechnical, dynamic and small-strain strength characterization. The flow chart of the experimental work has been presented in Fig. 3.1. Also, the various sources of materials, experimental standards used, and testing procedure were explained properly in a systematic manner.

3.2 SOURCE OF MATERIALS USED

3.2.1 Fly Ash

The coal fly ash has been collected from the Grasim industries private limited which is located in Renukoot, Uttar Pradesh, India (24° 12' 22.30" N, 83° 3' 13.68" E). The probable position of the Renukoot location in the map of India has been depicted in Fig. 3.2. The distance between Grasim industries and IIT(BHU) Varanasi campus is around 145 km and it comes under Sonbhadra district of Uttar Pradesh, India. The Grasim industries started its business in textile manufacturing but now becomes market leader of products such as pulp production, chemicals, fertilizers, insulators, cement etc. The Renukoot unit of Grasim industries is the manufacturer of caustic soda flakes which is majorly used in textile processing, paper, pulp, soap and detergent industries. They utilize coal to carry out various plant operations. The coal mines of Madhya Pradesh, Jharkhand and Chhattisgarh are the major source of coal in Grasim industries, and higher percentage of coal is imported from Singrauli (M.P). Anthracite, bituminous, sub-bituminous, and lignite are types of coal produces in these states of India.

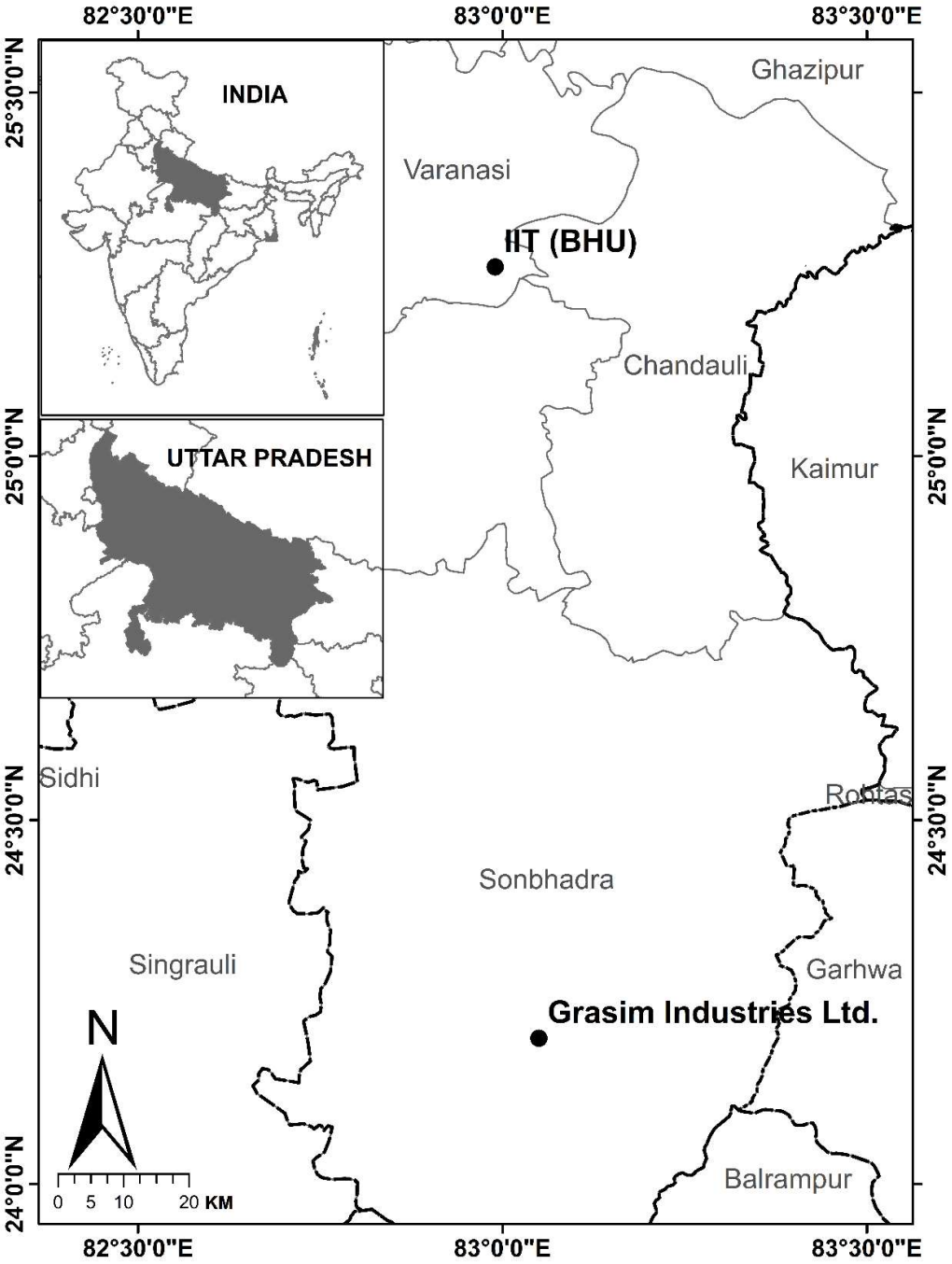

Fig. 3.2. Site locations of the considered materials.

3.2.2 Local Soil

The local soil as the name suggest has been collected from the campus of Indian Institute of Technology (Banaras Hindu University), Varanasi, Uttar Pradesh, India (25° 15' 44.28" N, 82° 59' 21.48" E). The probable position of the IIT(BHU) Varanasi location in the map of India has been depicted in Fig. 3.2. The reason behind the consideration of local soil is that the waste materials are usually applied over the existing ground surface which is more common in pavement applications, and it is applied in alternate layers of soil and waste material. Hence, it is significant to investigate the interaction of waste material with locally available soil.

3.3 EXPERIMENTAL PROGRAM

3.3.1 Chemical Characterization

3.3.1.1 Scanning Electron Microscope (SEM) Test

The surface morphology of the considered materials was explored using a Scanning Electron Microscope test. The SEM incorporates a beam of electron for the magnified images (less than nanometers) instead of light. The model of the machine used was EVO-Scanning Electron Microscope MA15/18 purchased from the company CARL ZEISS MICROSCOPY LTD with an EHT voltage of 20 kV and working distance of 11 mm for different magnification. In this experiment, a high intensity electron beam is allowed to fall through the anode, condenser magnet, scanning coil, and an objective lens into the sample. When the electron beam strikes the sample, then the back scattered electron, secondary electron, and X-rays are produced which will be detected using a secondary electron detector and the energy dispersive X-ray spectroscopy detector. The back scattered electrons are the electrons detected due to the elastic scattering, whereas secondary electrons are the electrons which are reflected from the atom's surface. These

scattering of electron is detecting by the secondary detectors results in the generation of high-resolution images using the analyzer.

However, the X-rays are produced when some electrons penetrated into the inner shell of the sample atom to knock off inner shell electrons because of which X-rays are released. The energy of the X-rays was detected by the energy dispersive X-ray spectroscopy detector that ultimately results in the elemental composition of the sample simultaneously. This test helps in both surface morphology and elemental composition of the sample in the same experimental assembly.

3.3.1.2 X-Ray Diffraction (XRD) Test

The X-ray diffraction test is conducted to determine the crystallinity and the structure of the solid samples. Basically, it is based on the Bragg's law principle. The Bragg's law can be expressed in the following equation.

$$n\lambda = 2d \sin\theta \tag{3.1}$$

Where, λ is the wavelength of the incident X-ray beam, d is the distance between the atom in a crystal, θ is the angle of incidence equals to the angle of diffraction, and n is an integer.

The X-rays are the incident on the sample and the diffraction of X-rays from the electrons of the atom present in the sample are detected without changing the wavelength. These incident and diffracted wave observations were plotted between intensity versus 2θ. These particular peaks were matched with standard available data so that its structure can be identified that will help in the determination of different minerals. The interpretation of the obtained XRD pattern was carried out using JCPDS-International Centre for Diffraction Data cards.

The X-ray diffraction test was performed using the facility available at Central Instrument Facility (CIF), IIT(BHU), Varanasi. The model of the equipment used was Rigaku Smart Lab 9kW Powder type (without χcradle) purchased from the company RIGAKU Corporation. The compounds present in the fly ash were detected with a radiation source of Cu-Kα of wavelength (λ) = 1.540 Å at 40 kV and 35 mA. The entire analysis was carried out in 2θ ranging from 20° to 80° with a step size of 0.02° and the scanning speed was set at 1° per min.

3.3.1.3. X-Ray Fluorescence (XRF) Spectroscopy

The qualitative and quantitative elemental composition of the material is usually evaluated by X-ray Fluorescence spectroscopy. It is a non-destructive test which works on the principle of absorption of fluorescence of X-ray from the specimen. In this test, the primary source of X-ray is focused on the sample and the florescent X-ray emitted from the sample is detected using a detector. Every element has its own emitting nature of florescent X-ray through which it can be identified. Basically, due to the illumination of X-ray, some electrons excited and jump to the next orbital level which will be fulfilled by another electron by releasing a fluorescent X-ray. The measurement of this energy helps in the identification of a particular element and its percentage. This test was conducted at CSIR-Institute of Minerals and Materials Technology (IMMT), Bhubaneswar with a Zetium XRF spectrometer (Malvern Panalytical, The Netherlands) having maximum capacity of 4 kW.

3.3.1.4 Potential of Hydrogen (pH)

The pH of soil can be determined conforming to the Indian standard IS 2720 (Part 26) (2002). There are two methods available for pH determinations a) electrometric method, and b) colorimetric method. The soil passing through 425 microns sieve was

taken for the test. Then, 30 gm of soil was mixed in 75 ml of distilled water in a beaker of 100 ml capacity, which was allowed to stand for 1 hour with occasional stirring. After that, the pH measuring electrode was calibrated using the buffer solution as per the instruction given by the manufacturer. This calibrated electrode was inserted inside the solution that directly display the pH value of the solution. The process was repeated with proper cleaning of the electrode using distilled water.

3.3.2 Geotechnical Characterization

3.3.2.1 Specific Gravity

The specific gravity of soil can be determined using density a bottle or pycnometer. This test has been performed by conforming to the Indian standard IS 2720 (Part 3) (1989). This test was carried out by taking 10–20 gm of the oven dried soil using a density bottle. Initially, the weight of the empty density bottle (W_1) and the bottle filled with soil (W_2) was taken. After that, sufficient amount of water was added in the density bottle and subjected to a vacuum pump to remove the entrapped air for 10 min. Then the bottle was completely filled with water till the top and the weight (W_3) was taken. Then the density bottle was cleaned properly, and filled with water, and the weight (W_4) was taken. The specific gravity of soil and ash sample was calculated using the equation mentioned below.

$$G = \frac{W_2 - W_1}{(W_4 - W_1)(W_3 - W_2)} \tag{3.2}$$

3.3.2.2 Grain Size Distribution

The grain size distribution is a very significant geotechnical laboratory test that helps in the exact classification of the soil type. This test was performed by arranging the different size of sieves in decreasing order from top to bottom conforming to the Indian

standard IS 2720 (Part 4) (1985). The standard sequence of sieves are 4.75 mm, 2 mm, 1 mm, 0.425 mm, 0.3 mm, 0.15 mm, 0.090 mm, and 0.075 mm respectively. In the present study, wet sieve analysis was performed by washing the known amount of soil with water through a 75-micron sieve. After washing, the residue left over 75-micron and passed fine particles was kept in an oven to make it completely dry prior to the test. Then particle size analysis was done only for the residue left over 75-micron in order to determine the percentage of particle size between 4.75 to 0.075 mm. The above-mentioned sieve arrangements with pan at the bottom was set on a sieve shaker with soil at the top and subjected to sieving for 10 min. The percentage weight retained on particular sieve was noted. Then the graph between percentage finer and sieve size was plotted. Whereas to determine the contribution of silt and clay size particle (0.075 mm to < 0.002 mm), the passed sample through 75-micron was collected (50 grams) and treated with deflocculating agents to make the solution of 1000 ml with the help of water. Using this solution, the Hydrometer analysis was performed through which the diameter of the particle and percentage fines was evaluated theoretically.

3.3.2.3 Atterberg Limit

The Atterberg limit test (liquid limit, plastic limit and shrinkage limit) of the local soil and fly ash was carried out as per the IS 2720 (Part 5) (1985). The liquid limit of local soil and fly ash was determined through the Casagrande liquid limit device and Fall cone penetrometer respectively. The liquid limit is the water content corresponding to the consistency which needs 25 numbers of blows (Casagrande apparatus). Similarly, the liquid limit in fall cone method is the water content corresponding to 20 mm penetration of the cone. Whereas plastic limit defined as the water content corresponding to the 3 mm diameter soil thread when it starts crumbling. In the same way, shrinkage limit was determined only for the plastic soil by filling an open cylinder

at consistency higher than liquid limit, and allowing for air and oven drying. The change in volume of the shrink soil was used to determine the shrinkage limit of the local soil.

3.3.2.4 Standard Proctor Test

The standard Proctor test is also known as light compaction test was performed to determine the maximum dry density (MDD) and optimum moisture content (OMC) of the soil and fly ash samples as per IS 2720 (Part 7) (1980). The compaction test was carried out by taking 5 kg of oven dried soil sample and mixing it with trial water content. The soil mixture was then placed in the Proctor mould and compacted in three layers, receiving 25 blows per layer from a height of 30 cm with a 2.5 kg rammer. Then the compacted weight of soil was taken for the estimation of bulk unit weight and also some representative sample was kept for the moisture content determination. The moisture content at a particular trial water content helps in the estimation of dry unit weight of the sample. This step was repeated for increasing percentage of moisture content unless the compacted weight of soil starts decreasing. Then the plot between dry unit weight and moisture content was used for obtaining the maximum dry unit weight and optimum moisture content of the samples.

3.3.2.5 Falling Head Permeability Test

The constant head permeability test is generally adopted for coarse grained soil (Sand) whereas the falling head permeability test is considered for fine grained soil (fine silt and clay). In the present study, the considered materials are of fine-grained nature, hence falling head permeability test has been used to determine the permeability of soil and fly ash samples. The tests were performed using a rigid wall compaction mould permeameter as per IS 2720 (Part 17) (1986). The oven dried soil sample of 2.5 kg was mixed with known amount of water to achieve the desired density. Then the soil mixture

was compacted in three layers using a 2.6 kg hammer. The sample was then saturated with de-aired water. The inlet nozzle of the mould was connected to the standpipe, and water flow was allowed until a steady flow was achieved. The time interval for a head fall in the standpipe was then recorded. The coefficient of permeability of the soil can be calculated using the equation given below.

$$k_T = \frac{aL}{A\,(t_f - t_i)} \log_{10} \frac{h_1}{h_2} \tag{3.3}$$

Where, k_T: coefficient of permeability, L: length of the specimen, D: diameter of the specimen, a: area of the stand pipe, h_1 & h_2 is the head in the stand pipe, and t_f & t_i is the time interval.

3.3.2.6 Triaxial Shear Test

To determine the shear strength parameters of the considered soil and fly ash, the static triaxial tests were conducted under three conditions, i.e., Unconsolidated Undrained (UU), Consolidated Undrained (CU), Consolidated Drained (CD), and are explained below.

3.3.2.6.1 Unconsolidated Undrained (UU) Triaxial Test

The triaxial test is conducted in four stages, i.e., a) mounting of the sample, b) saturation of the sample, c) consolidation of the saturated sample, and d) shearing of the sample. For the Unconsolidated Undrained (UU) triaxial test, the samples were unconsolidated and drainage was not allowed during the shearing process. The static UU triaxial tests were conducted according to the IS 2720 (Part 11) (1993). In this test, a cylindrical sample having a length/diameter ratio equal to 2 (100mm length and 50mm diameter) has been prepared using the moist tamping method and subjected to progressive static loading for three confining pressures (σ_3) 50 kPa, 100 kPa, and 150 kPa.

3.3.2.6.2 Consolidated Undrained (CU) Triaxial Test

When the drainage of water is allowed during the consolidation phase and stopped during the shearing phase, then it is considered as the consolidated undrained triaxial condition. The static CU triaxial tests were conducted according to the IS 2720 (Part 12) (1981). The prepared sample was kept for saturation involving the confining pressure and back pressure assembly. The level of saturation was determined by estimating the Skempton's B parameter (Skempton 1954). The saturation process was continued until the Skempton's Pore Pressure Parameter B ($B = \Delta u/\Delta\sigma_c$, Δu = change in pore pressure, and $\Delta\sigma_c$ = change in confining pressure) reaches almost 0.99. Once the sample was completely saturated, it was consolidated to a desired effective confining pressure, and the volume change was recorded. Then the shearing was carried out under the confining pressure of 50, 100, and 150 kPa without allowing drainage during shearing.

3.3.2.6.3 Consolidated Drained (CD) Triaxial Test

The static CD triaxial tests were conducted according to the IS 2720 (Part 12) (1981). Here, also the samples were tested under the confining pressures of 50, 100, and 150 kPa. The sample preparation, saturation, and consolidation steps were similar to the CU triaxial test. In this test, the drainage of water is allowed during both the phase of consolidation and shearing stage.

3.3.2.7 California Bearing Ratio (CBR) Test

The CBR tests were carried out according to the IS 2720 (Part 16) (1987). The CBR tests were conducted for both soil and fly ash samples under the unsoaked and soaked conditions. The soaking period of 96 hours was maintained before going for soaked CBR tests.

3.3.3 Dynamic Characterization

3.3.3.1 Cyclic Triaxial Test

3.3.3.1.1 Description of the Equipment

A computerized semi-automated triaxial testing equipment with the facility of both static and dynamic testing, supplied by M/s. HEICO, New Delhi, India, was used for this study. The equipment consists of a submersible load cell of capacity ±5 kN with an accuracy of 0.001 kN and a displacement transducer of ±50 mm (with 0.01 mm accuracy) and ±10 mm (with 0.01 mm accuracy). The pore pressure transducers have a range of 0–2,000 kPa and an accuracy of 1.0 kPa fitted at the back side of the base of the triaxial cell. The load frame can accommodate triaxial cells with sample sizes ranging from 38 mm to 100 mm in diameter with a length-to-diameter ratio of 2:1. Both stress-controlled and strain-controlled tests can be performed using a hydraulic-controlled loading system. A hydraulic power supply (power pack) is provided to provide the required flow and pressure for hydraulic actuator actuation. The pneumatic control panel is a component of the cyclic triaxial system that ensures accurate confining and back pressure using the compressed air produced by the air compressor. The cell pressure and back pressure are controlled manually through precise regulators. By using an external input, the equipment can vary the frequency range from 0.01 Hz to 10 Hz with various waveforms such as sine, triangular, rectangular, square, or any other. The photographic view of the equipment and accessories used is shown in Fig. 3.3.

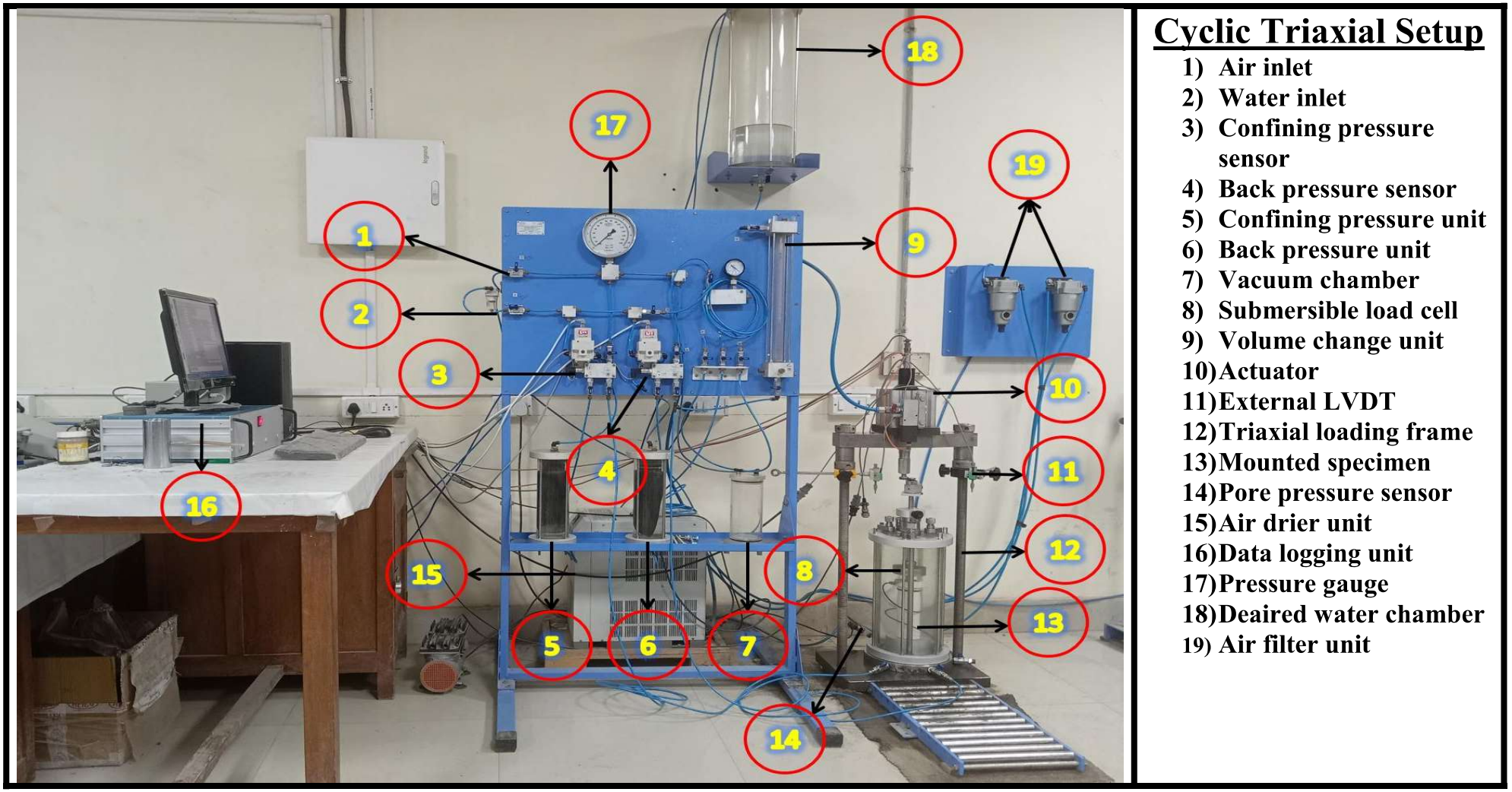

Fig. 3.3. Pictorial illustration of cyclic triaxial test apparatus.

3.3.3.2 Sample Preparation for Cyclic Triaxial Test

Practically, it is very challenging to maintain the structural orientation, moisture content, and void ratio of the undisturbed specimen collected from the site. But undisturbed specimen exhibits higher strength as compared to the reconstituted specimen (Townsend 1978). Hence, the sample prepared in the laboratory is more preferred for the static/dynamic characterization of soil. Most commonly used sample preparation methods in the past studies are given below:

- Pluviation through air
- Pluviation through water
- Moist rodding
- Moist tamping
- Dry rodding
- Horizontal vibration under low or high frequency
- Vertical vibration under low or high frequency
- Moist tamping
- Slurry deposition
- Under compaction method
- Wet pouring method

These methods were used to prepare the cylindrical specimen for the determination of liquefaction potential of soil. Ladd (1974) considered dry vibration and wet tamping method for three different sand samples and found high liquefaction potential by a wet tamping method with the percentage variation of 100%. In the same way, Mulilis et al. (1975) investigated eleven various sample preparation techniques on Monterey sand. They concluded that the pluviation through air produced a very weakest specimen

whereas the strongest specimens were prepared by the moist vibration technique in terms of cyclic strength. The resistance to the liquefaction potential of soil is primarily dependent on the use of sample preparation technique that ultimately a function of type of soil used. The fundamental problems associated with the above methods are 1) the segregation of different size of particles, 2) difficulty in achieving the desired dry density, 3) none of the methods can be applied to all types of soil. The reason behind the segregation is that the large particles possess higher velocity of settlement or free fall than that of the small size particles which results in the early deposition of large particles. The segregation phenomena during sample preparation have been witnessed by several researchers (Amini and Sama 1999; Yoshimine and Koike 2005). The limitations of these methods were highlighted by Ladd (1978) and rectified by introduction a new sample preparation method known as an under-compaction method. The under-compaction method addresses the densification of the lower layer due to the compaction of the above successive layers as well. This densification problem was eliminated by under compacting the initial layers at a lower density than the desired. Vucetic and Dobry (1988) prepared sample by the under-compaction method and observed a uniform sample of the reconstituted silty sandy soil specimens. Vaid and Negussey (1988) observed the uniform sample preparation of sand without fines by pluviation through air and water as compared to the moist tamping and vibration method. The height of the sample pouring and other arrangements makes the pluviation technique little complex. Jang and Frost (1998) analyzed the soil structure of the sample digitally by employing optical microscope, found stable and uniform standard deviation of void ratio in the case of a pluviation method than that of the moist tamping. Amini and Chakravrty (2003) recommended to use the air pluviation method for the sample preparation of sand to gravel size of particles containing without fines. Also, found

similar types of samples prepared from moist vibration and moist tamping technique. The sample prepared by sedimentation method, water pluviation, and the slurry deposition method are closer to the natural soil deposits. From the above discussion, this can be concluded that the aforementioned methods are primarily used for the preparation of sand and silt size of particles. These are not appropriate for the sample preparation of coarse-grained containing fines or fine-grained soil. The sedimentation method, water pluviation, and slurry deposition method requires much time (approx. 24 hour) for the stability of the first layer, again same time for the second layer and so on (Dingrando et al. 2013). The moist tamping method is the only method that can be used to compact any types of soil at any desired density. The moist tamping method has been implemented by various researchers for liquefaction studies (Koester 1992; Amini and Qi 2000; Bradshaw and Baxter 2007; Mohanty and Patra 2014). Hence, the moist tamping method combined with the concept of the under-compaction would definitely results in the preparation of the uniform homogeneous and stratified soil sample. In the moist tamping method, the sample preparation is generally carried out in multiple layers with equal number of blows. But, for specimens with diameters smaller than 102 mm, the maximum thickness of the layers shouldn't be more than 25 mm (Ladd 1978).

In the present study, the considered soils are predominantly consisting of fine-grained soil particles. Therefore, the moist tamping technique with the concept of the under-compaction has been employed for the sample preparation of homogeneous and stratified soil-ash samples. Here, the cylindrical sample having a diameter of 50 mm and a length of 100 mm has been considered for the dynamic characterization of the soil and fly ash samples. The pictorial representation of the sample preparation of both the sample has shown in Fig. 3.4.

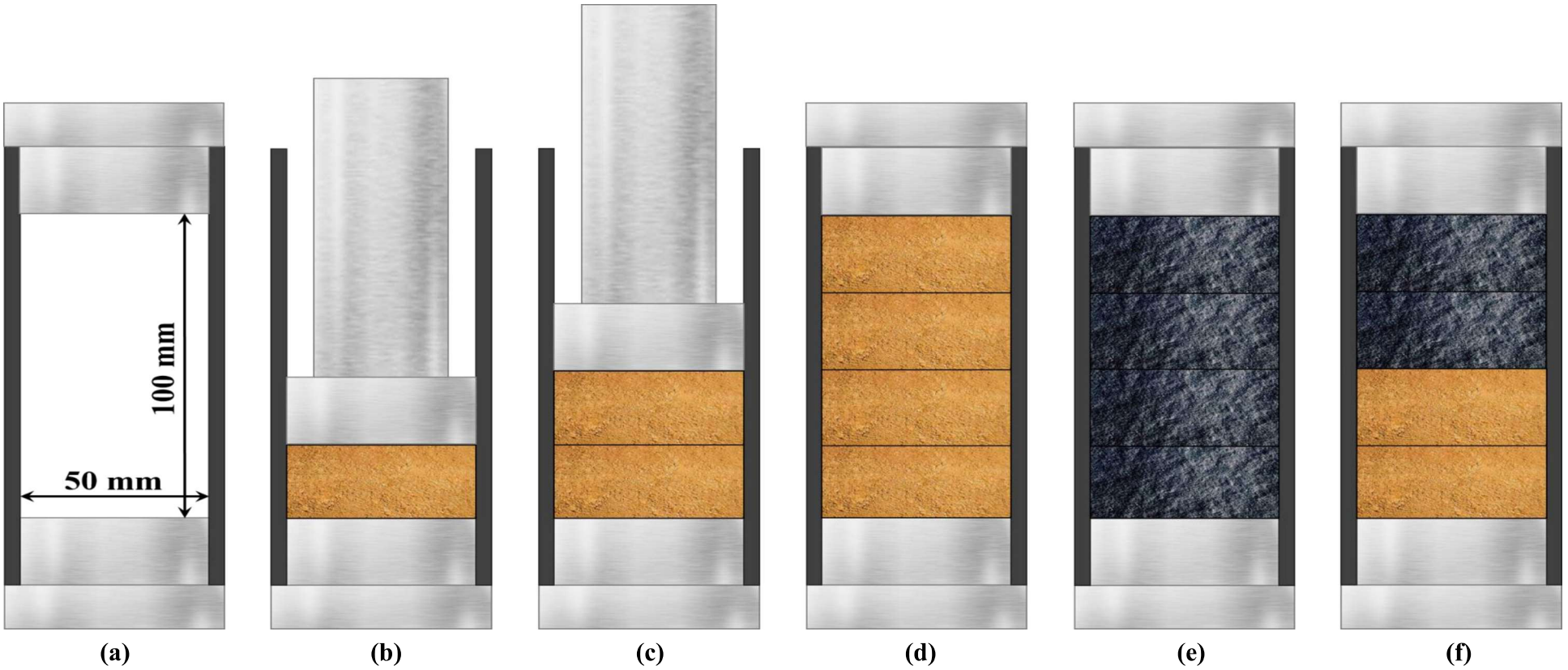

Fig. 3.4. Illustration of sample preparation, (a) sample preparation mold, (b) compaction of first layer of local soil, (c) compaction of second layer, (d) final compacted form of local soil, (e) final compacted form of fly ash, (f) final compacted form of stratified soil-ash deposit.

3.3.3.3 Testing Procedure of Cyclic Triaxial Test

In the present study, the homogeneous and stratified soil-ash samples were tested to determine the dynamic soil parameters (shear modulus and damping ratio) as well as to evaluate its liquefaction potential when subjected to cyclic loading. Here, all the advanced cyclic triaxial tests were executed under consolidated undrained (CU) condition with a cylindrical specimen of diameter 50 mm and height 100 mm. The cylindrical specimen was prepared by following the moist tamping technique. Then the filter paper and porous stones were placed on top and bottom of the sample. After this rubber membrane was pulled over the sample and the assembly was sealed with an O-ring. There are generally three steps in the triaxial test after preparation and mounting of the sample, i.e., saturation, consolidation, and shearing. Once the sample was mounted in the triaxial cell, the saturation process was continued by increasing the back pressure at regular intervals while keeping the effective confining pressure at 20 kPa and the Skempton's pore water parameter (B) ($B = \Delta u/\Delta\sigma_c$, Δu = change in pore pressure, and $\Delta\sigma_c$ = change in confining pressure) was periodically monitored until a value of 0.99 was achieved indicating that the specimen was essentially saturated.

Once the saturation was achieved up to 99%, it was isotopically consolidated to a desired effective confining pressure. If there is no variation in the volume change readings and the pore pressure remains stable during that period, the consolidation process is assumed to be completed. After the consolidation process, the sample was subjected to strain-controlled cyclic loading in the vertical direction using a hydraulic actuator. The cyclic shearing of the homogeneous and stratified soil-ash samples were carried out in the laboratory under different relative compactions (95, 97, and 99%), confining pressures (100, 80, & 70 kPa), frequencies (1.0, 0.5 & 0.3 Hz), and cyclic shear strain amplitudes (0.3-1.5%) as per the ASTM D5311 (1992) and ASTM D3999

(1996). All samples were cyclically loaded until they failed, i.e., the excess pore pressure ratio attained one for CU cyclic triaxial tests. The data acquisition system was used to record the axial deformation, confining pressure, pore water pressure, cyclic load, and the number of cycles.

The dynamic shear modulus (G) and damping ratio (D) are the fundamental dynamic properties of soil. The dynamic shear modulus is a vital property of soil for designing any structure in seismic regions for both high and low strain conditions. A typical hysteresis curve for soil is presented in Fig. 3.5(a) (Sitharam et al. 2004). The hysteresis loop provides an aid for the calculation of Young's modulus (E) from Eq. (3.4). The Eq. (3.5) helps in the evaluation of G with E, axial strain (ε), and Poisson's ratio (ν). A value of 0.5 is generally adopted for the Poisson's ratio in saturated undrained samples (Rollins et al. 1998). The amount of energy dissipated under cyclic loading condition is termed as the damping ratio (D), which can be evaluated by using Eq. (3.6).

$$E = \sigma_d/\varepsilon \tag{3.4}$$

$$\gamma = (1+\nu)\varepsilon \text{ and } G = E/2(1+\nu) \tag{3.5}$$

$$D = A_L/(4\pi A_T) \tag{3.6}$$

where, A_L = area covered by the hysteresis curve; and A_T = area of the triangular portion.

Also, the specimen mounting of cyclic triaxial test starting from the sample preparation to membrane stretching and mounting inside the triaxial cell has been shown in Fig. 3.6. The saturation of the specimen is a time consuming process which depends primarily on the coefficient of permeability and void ratio. The low

permeability soil (clay) takes a longer period of time for the saturation whereas high permeability soil (sand) saturates in a short period of time. Therefore, fly ash saturates faster than the stratified soil followed by local soil. Except sample preparation, all the mounting, saturation, and testing procedure are same for both homogeneous and stratified soil-ash deposit.

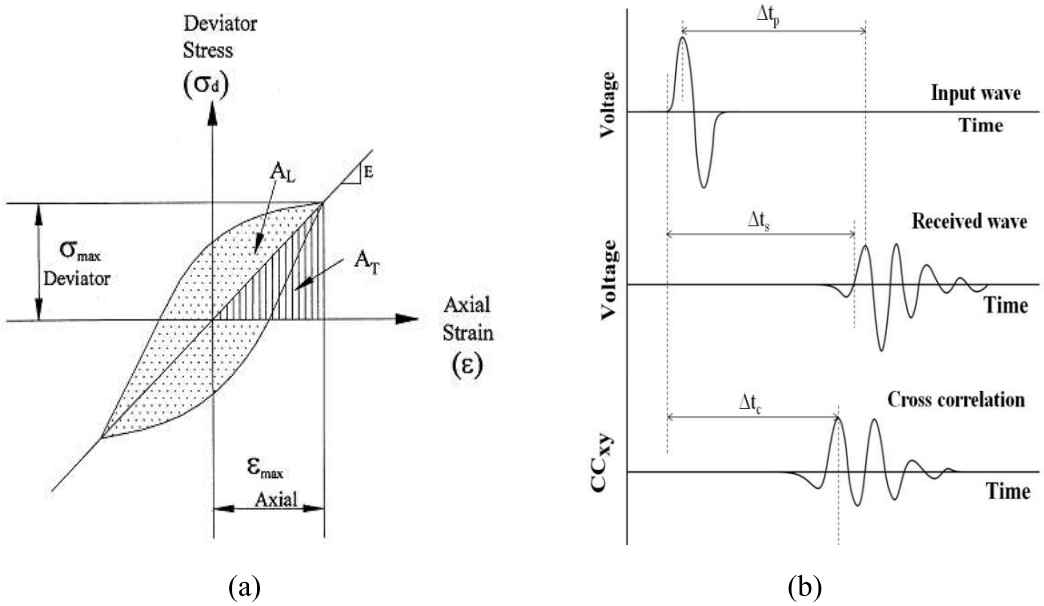

(a) (b)

Fig. 3.5. (a) Hysteretic stress–strain relationship for cyclic loading (Sitharam et al. 2004) and (b) Travel time determination using time domain technique. (Kawaguchi et al. 2016)

(a) (b) (c) (d) (e) (f)

Fig. 3.6. Pictures showing various stages in sample preparation for cyclic triaxial test: (a) Fly ash sample (b) Prepared specimen (c) Specimen with rubber membrane (d) Specimen with top piston assembly (e) Specimen with triaxial cell assembly and (f) Specimen subjected to confining pressure.

3.3.4 Small-Strain Shear Modulus Characterization

3.3.4.1 Bender Element Test

The bender element test is based on the principle of piezoelectricity, which was first invented by Jacques and Pierre Curie in 1880. The concept of piezoelectricity was first time used to find the small-strain shear modulus (Shirley 1977; Shirley and Hampton 1978). According to this piezoelectric property, when an electric voltage is activated to one end of the piezoceramic element, it generates mechanical excitation. These generated mechanical waves again excite the other end of the element that results in the generation of electric voltage. Basically, in this test, it is required to determine the time needed by the electrically excited wave to travel from one end to other ends of the specimen connected to piezoceramic elements. It is commonly used to find the small-strain shear modulus by applying the following expression.

$$G_{max} = \rho V_s^2 = \rho(\frac{L}{\Delta t})^2 \quad (3.7)$$

where, ρ = bulk mass density of the material (kg/m^3); Vs = velocity of the shear wave (m/sec), L = travel length of the wave and Δt is the travel time taken by the waves. Eq. (3.7) is applicable for the case when characteristic frequency is less than 1.1 times the excitation frequency (Youn et al. 2008). The measured travel time of the waves is an essential factor in the bender element test, which can be determined with the help of an oscilloscope. Either method of time domain or frequency domain can be employed to estimate the travel time of the waves.

In a time-domain analysis, there are different approaches for the measurement of travel time, such as start-to-start (S.S.), peak-to-peak (P.P.), and cross-correlation (C.C.) (Viggiani and Atkinson 1995; Yamashita et al. 2009; Kawaguchi et al. 2016). In the start-to-start (S.S.) approach, travel time is the time taken by the wave from the starting position of the transmitting wave to the starting position of the receiving wave (Δt_s). Similarly, in the peak-to-peak (P.P.) approach, travel time is the time taken by the wave from the peak of the transmitting wave to the peak of the receiving wave (Δt_p). The cross-correlation method is the measure of similarity between the transmitted and received waves as a time difference function. It can be determined by using the following formula.

$$CCxy\,(\tau) = \lim_{T=\infty} \frac{1}{T} \int_0^T X(t)Y(t+\tau)dt \quad (3.8)$$

where, $X(t)$= input signal, $Y(t)$ =output signal, T = total time travel and τ = time shift between input and output signal. All the time domain methods are explained in graphical form in Fig. 3.5(b). The identical time lag is determined by any of the three

methods (S.S, P.P, and C.C) when the input frequency of a wave is equal to the output frequency of the wave (Viggiani and Atkinson 1995; Yamashita et al. 2009).

In the frequency domain method, the travel time is determined with the help of phase velocity, and it is based on the assumption that the input wave frequency is equal to the output wave frequency. The phase velocity can be obtained from the cross phase spectrum of the generated and received waves (Viggiani and Atkinson 1995). The travel time difference estimated by the frequency domain method shows a significant variation with that obtained by the time domain method. Hence, time domain analysis is preferred to determine the time delay. The travel time has been determined by first arrival (start to start) method which is suggested by Georgetti and Rodrigues (2013) as reliable for the calculation of shear wave velocity. In order to eliminate the near-field effect in shear wave velocity, the distance/wave length (L/λ) should be kept above 3 (Georgetti and Rodrigues 2013) or above 2 (Youn et al. 2008).

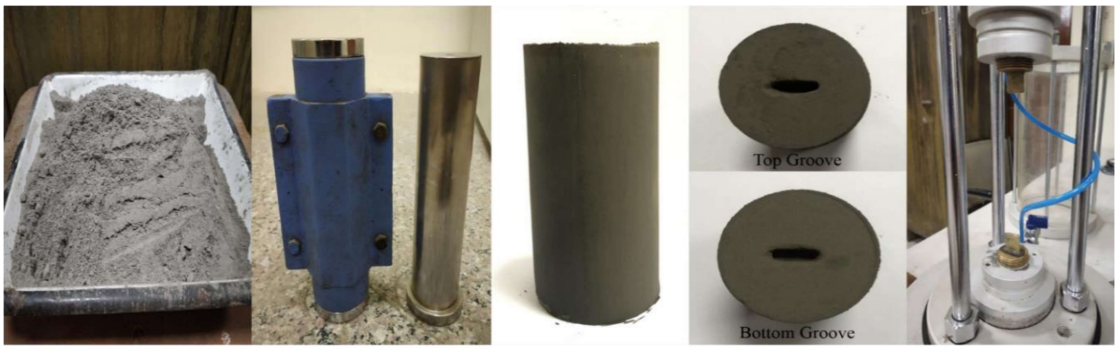

(a) (b) (c) (d) (e)

(f) (g) (h)

Fig. 3.7. Pictures showing various stages in sample preparation for bender element test: (a) Fly ash sample (b) Mould for sample preparation (c) Extracted specimen (d) Top and bottom groove of bender element (e) Bender element without specimen (f) Specimen kept on bottom element (g) Mounted specimen and (h) Mounted specimen with confining pressure.

The bender element is a non-destructive test which comes under very small shearing strain range. As discussed above, it is used to determine the maximum shear modulus that will be employed for the evaluation of the modulus reduction curve. The complete sample preparation, sample size and mounting is same as that of the cyclic triaxial test except grooving on top and bottom of the specimen. The bender element has a length of 13 mm, width of 13 mm, and thickness of 4 mm. The groove of size same as bender element's transmitter and receiver will be done on top and bottom with the help of sharp object. After the preparation of groove, the bender elements should be

carefully inserted from the top and bottom so that proper contact can be established. The complete sample preparation, grooving, and mounting of the specimen on bender element has been shown in Fig. 3.7. The bender element test was performed as per the ASTM D2845 (2000).

3.3.5 Testing Program

All the above discussed experiments such as morphological, minerological, chemical, geotechnical properties, and sample preparation were done for the classification and identification of the samples in terms of physical, chemical, and geotechnical characterization. Since the objective of the present study is to investigate the dynamic properties and liquefaction potential behavior of the materials under wide shear strain condition. Hence, once the basic experiments were completed, the considered materials were planned to test by considering different dynamic influencing parameters. These influencing parameters are relative compaction, effective confining pressure, frequency of loading, the amplitude of shear strain. For sustainable functioning of fly ash applied in pavement subgrade or embankment material, it must be densified to a relative compaction between 95 to 100% of the maximum dry density (MDD) (ASTM-D698-12, 2012). Observing the difficulty in achieving the desired densification of fly ash, it is recommended to compact the fly ash below the optimum moisture content (OMC) (ACAA, 2003). Thus, in order to cover this range of density, the relative compaction between 95% to 99% has been chosen so that its performance under low and high density can be analyzed.

The coal ash usually dumped in loose form and their continuous dumping results in the dump height of 10-30 m (Singh et al., 2008). Sand exhibits confining pressure between 41-124 kPa for the overburden height of 2-7 m (Figueroa et al., 1994).

Similarly, fly ash would require overburden height of 10-40 m to exert confining pressure between 100-400 kPa. But, bottom/fly ash filled embankment up to a height of 3-5 m will generate confining pressure in the range of 10-50 kPa (Chandra et al., 2016). Hence, in order to cover the dynamic behavior of the existing height of ash pond deposits and its application in different field of Civil engineering, the confining pressure between 70-100 kPa has been considered here. Also, these confining pressures are very frequently used by past researchers. Therefore, these confining pressures were introduced in order to compare the current outcome with the past results more effectively.

Dobry and Abdoun (2015) performed strain-controlled cyclic triaxial test as well as a centrifuge model test, to determine the shear strain required to activate liquefaction. They observed that the shear strain needed in the case of silty sand was approximately 0.4 to 3% under an earthquake of magnitude Mw: 7.5. Moreover, Tsukamoto et al. (2004) also performed a similar study based on real-time seismic data and found the initiation of liquefaction activity at 3.75% cyclic shear strain. Since the presently considered materials are showing high dominance in silt/sand size particle. Therefore, the shear strain of 0.3, 0.6, 0.9, 1.2, & 1.5% has been taken for the present study. The seismic events are random shaking movements that did not follow a uniform frequency, but in the cyclic triaxial test a single frequency of loading is considered at a particular time. In order to incorporate different loading frequencies, the cyclic loading frequency (f) of 0.3, 0.5, and 1.0 Hz has been considered.

Therefore, considering these influencing parameters, the consolidated undrained triaxial tests were performed in cyclic triaxial setup and bender element assembly. The detailed schematic description of the testing program for the cyclic triaxial and bender element test has been shown in Fig. 3.8.

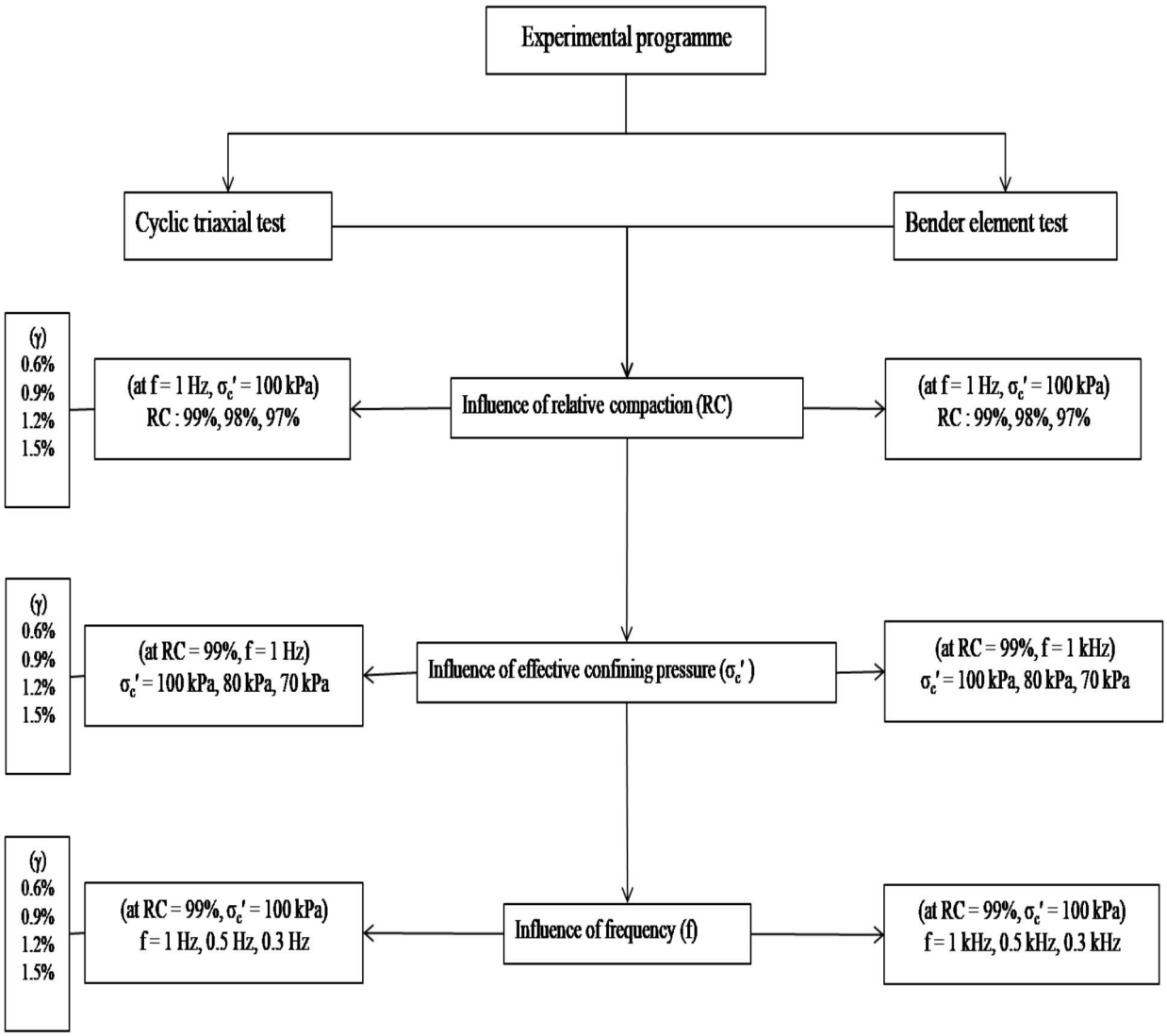

Fig. 3.8. Schematic description of testing program for the cyclic triaxial and bender element test.